5416 *Inorg. Chem.* **1995**, *34*, 5416–5423

Solution Study of the Ambient Temperature Monomer–Dimer Equilibrium $Th_2(OR)_8 \rightleftharpoons 2Th(OR)_4$ ($R = CH\text{-}i\text{-}Pr_2$) and X-ray Crystal Structures of $Th_2(OCH\text{-}i\text{-}Pr_2)_8$, $Th(OCH\text{-}i\text{-}Pr_2)_4(quin)$, and $ThI(OCH\text{-}i\text{-}Pr_2)_3(py)_2$

David M. Barnhart,[1a] David L. Clark,[*,1b] John C. Gordon,[1b] John C. Huffman,[1c] John G. Watkin,[*,1b] and Bill D. Zwick[1d]

Chemical Science and Technology (CST) Division and Nuclear Materials Technology (NMT) Division,
Los Alamos National Laboratory, Los Alamos, New Mexico 87545, and Molecular Structure Center,
Indiana University, Bloomington, Indiana 47405

Received May 4, 1995[⊗]

The thorium metallacycle $[(Me_3Si)_2N]_2\overline{Th[N(SiMe_3)(SiMe_2CH_2}]$ (**1**) reacts with 4 equiv of 2,4-dimethylpentan-3-ol (diisopropylmethanol) in toluene at room temperature to produce dimeric $Th_2(OR)_8$ (**2**) ($R = CH\text{-}i\text{-}Pr_2$). ^1H NMR spectra of **2** in noncoordinating solvents indicate a monomer–dimer equilibrium in solution at ambient temperatures between **2** and its monomer $Th(OR)_4$ (**3**). Thermodynamic parameters for the equilibrium process are $\Delta H° = 17$ kcal mol^{-1}, $\Delta G° = 5$ kcal mol^{-1}, $\Delta S° = 40$ cal mol^{-1} K^{-1}. Addition of Lewis bases such as DME (DME = 1,2-dimethoxyethane), pyridine or quinuclidine to solutions of **2** results in the formation of the five- and six-coordinate mononuclear adducts $Th(OR)_4(DME)$ (**4**), $Th(OR)_4(py)_2$ (**5**), and $Th(OR)_4(quin)$ (**6**), respectively. Reaction of **5** with 1 equiv of Me_3SiI produces the monoiodide derivative $ThI(OR)_3(py)_2$ (**7**). Compounds **2**–**7** have been characterized by ^1H NMR and IR spectroscopy, by elemental analysis, and, in the case of **2**, **6**, and **7**, by single crystal X-ray diffraction studies. $Th_2(OCH\text{-}i\text{-}Pr_2)_8$ (**2**) exhibits a dimeric structure in which the Th_2O_8 core can be viewed as two ThO_5 trigonal bipyramids joined along a common axial-equatorial edge. Terminal Th–O distances average 2.154(11) Å while bridging Th–O distances are significantly longer at 2.436(11) Å (average). $Th(OCH\text{-}i\text{-}Pr_2)_4(quin)$ (**6**) displays a trigonal bipyramidal geometry with the quinuclidine ligand occupying an axial site. Th–O distances average 2.165(17) Å while the Th–N distance is 2.712(11) Å. $ThI(OCH\text{-}i\text{-}Pr_2)_3(py)_2$ (**7**) exhibits a facial pseudooctahedral geometry in the solid state, with Th–O and Th–N distances averaging 2.136(8) and 2.746(9) Å, respectively, and a Th–I distance of 3.226(1) Å. Crystal data for **2** at −170 °C: monoclinic space group $P2_1/n$, $a = 12.115(2)$ Å, $b = 20.820(3)$ Å, $c = 13.002(2)$ Å, $\beta = 100.62(1)°$, $V = 3223.4$ Å^3, $d_{calcd} = 1.428$ g cm^{-3}, $Z = 2$. Crystal data for **6** at −70 °C: monoclinic space group Cc, $a = 18.778(3)$ Å, $b = 11.391(2)$ Å, $c = 20.538(3)$ Å, $\beta = 113.51(2)°$, $V = 4028.4$ Å^3, $d_{calcd} = 1.356$ g cm^{-3}, $Z = 4$. Crystal data for **7** at −70 °C: triclinic space group $P\bar{1}$, $a = 9.691(2)$ Å, $b = 11.739(2)$ Å, $c = 17.006(3)$ Å, $\alpha = 77.63(3)°$, $\beta = 75.34(3)°$, $\gamma = 72.41(2)°$, $V = 1764.1$ Å^3, $d_{calcd} = 1.624$ g cm^{-3}, $Z = 2$.

Introduction

Oligomerization of homoleptic metal alkoxide species is a common phenomenon[2] which is particularly prevalent in the chemistry of the f-block metals where large ionic radii allow for high coordination numbers about the metal center.[3] Thus it has been shown that lanthanide and actinide complexes containing less bulky alkoxide ligands such as methoxide, neopentoxide or isopropoxide show a strong tendency toward oligomerization, resulting in the isolation of dinuclear[4] or tetranuclear[5] complexes and higher oligomers.[6] Some of the structural types documented to date are shown schematically in **I**–**III**.

Over the last several years, there have been numerous reports of the use of sterically encumbered aryloxide and alkoxide ligands to control both the coordination number of the lanthanide or actinide metal center and the degree of oligomerization of the complex.[3,7] It has become apparent during this time that subtle changes in the steric demands of a ligand set can significantly alter the structural characteristics of a metal alkoxide complex. For example, the tris(aryloxide) complexes

---

[⊗] Abstract published in *Advance ACS Abstracts*, October 1, 1995.

(1) (a) LANL. Present address: Department of Chemistry, University of Washington, BG-10, Seattle, WA 98185. (b) LANL, Mail Stop C346. (c) Indiana University. (d) LANL, Mail Stop E510.

(2) (a) Bradley, D. C. *Chem. Rev.* **1989**, *89*, 1317. (b) Bradley, D. C.; Mehrotra, R. C.; Gaur, D. F. *Metal Alkoxides*; Academic Press: London, 1978. (c) Mehrotra, R. C. *Adv. Inorg. Chem. Radiochem.* **1983**, *26*, 269.

(3) (a) Mehrotra, R. C.; Singh, A.; Tripathi, U. M. *Chem. Rev.* **1991**, *91*, 1287. (b) Sattelberger, A. P.; Van der Sluys, W. G. *Chem. Rev.* **1990**, *90*, 1027.

(4) (a) Vaartstra, B. A.; Huffman, J. C.; Gradeff, P. S.; Hubert-Pfalzgraf, L. G.; Daran, J.-C.; Parraud, S.; Yunlu, K.; Caulton, K. G. *Inorg. Chem.* **1990**, *29*, 3126. (b) Toledano, P.; Ribot, F.; Sanchez, C. *Acta Crystallogr.* **1990**, *46C*, 1419. (c) Van der Sluys, W. G.; Huffman, J. C.; Ehler, D. S.; Sauer, N. N. *Inorg. Chem.* **1992**, *31*, 1316. (d) Hubert-Pfalzgraf, L. G.; El Khokh, N.; Daran, J-C. *Polyhedron* **1992**, *11*, 59.

(5) (a) Evans, W. J.; Sollberger, M. S.; Shreeve, J. L.; Olofson, J. M.; Hain, J. H., Jr.; Ziller, J. W. *Inorg. Chem.* **1992**, *31*, 2492. (b) Yunlu, K.; Gradeff, P. S.; Edelstein, N.; Kot, W.; Shalimoff, G.; Streib, W. E.; Vaartstra, B. A.; Caulton, K. G. *Inorg. Chem.* **1991**, *30*, 2317. (c) Barnhart, D. M.; Clark, D. L.; Gordon, J. C.; Huffman, J. C.; Watkin, J. G.; Zwick, B. D. *J. Am. Chem. Soc.* **1993**, *115*, 8461. (d) Barnhart, D. M.; Clark, D. L.; Gordon, J. C.; Huffman, J. C.; Watkin, J. G. *Inorg. Chem.* **1994**, *33*, 3939.

(6) (a) Bradley, D. C.; Chudzynska, H.; Frigo, D. M.; Hammond, M. E.; Hursthouse, M. B.; Mazid, M. A. *Polyhedron* **1990**, *9*, 719. (b) Helgesson, G.; Jagner, S.; Poncelet, O.; Hubert-Pfalzgraf, L. G. *Polyhedron* **1991**, *10*, 1559. (c) Andersen, R. A.; Templeton, D. H.; Zalkin, A. *Inorg. Chem.* **1978**, *17*, 1961. (d) Barnhart, D. M.; Butcher, R. J.; Clark, D. L.; Gordon, J. C.; Watkin, J. G.; Zwick, B. D. *New J. Chem.* **1995**, *19*, 503. (e) Poncelet, O.; Sartain, W. J.; Hubert-Pfalzgraf, L. G.; Folting, K.; Caulton, K. G. *Inorg. Chem.* **1989**, *28*, 263. (f) Evans, W. J.; Sollberger, M. S. *J. Am. Chem. Soc.* **1986**, *108*, 6095.

0020-1669/95/1334-5416$09.00/0

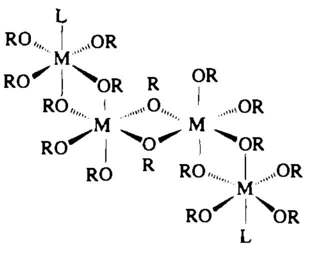

I (M = Th, R = *i*-Pr, L = py)[5d]

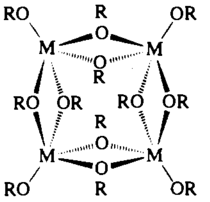

II (M = Nd, R = CH_2-*t*-Bu)[5c]

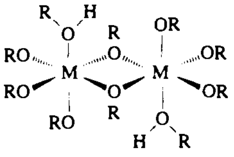

III (M = Ce, R = *i*-Pr)[4a]

M(O-2,6-*t*-$Bu_2C_6H_3)_3$ (M = La–Lu, U) exist both in the solid state and in solution as discrete three-coordinate monomeric species.[7a,b] However, decreasing the steric bulk of the substituents in the 2,6-positions of the aryloxide ligand from *tert*-butyl to isopropyl allows the isolation of the dimeric complexes [M(O-2,6-*i*-$Pr_2C_6H_3)_3]_2$, which are held together both in the solid state and in solution by π-arene interactions as shown schematically in **IV**.[7b,8]

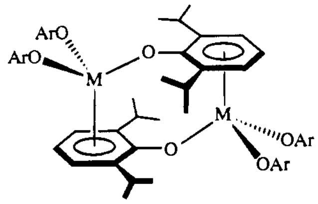

IV (M = La, Nd, Sm, Er, U)

In the case of alkoxide complexes, we have noted the use of sterically demanding alkoxide ligands such as *tert*-butoxide,[9] triphenylmethoxide and -siloxide,[10] di-[11] and tri-*tert*-butylmethoxide,[12] and fluorinated derivatives thereof.[13] In light of the significant structural changes noted above upon changing from *tert*-butyl to isopropyl substituents, we set out to investigate the structural properties of f-element alkoxide complexes ligated primarily by the diisopropylmethoxide ligand. We have previously reported the isolation and structural characterization of discrete dimeric neodymium complexes of the type $Nd_2(OCH$-*i*-$Pr_2)_6L_2$ (L = THF, pyridine), and also $Nd_2(OCH$-*i*-$Pr_2)_6L$ (L = DME) in which DME ligands bridge between adjacent dimeric units thus producing an infinite chain structure.[14] Additionally, we have found that the homoleptic thorium alkoxide complex $Th_2(OCH$-*i*-$Pr)_8$ exists in the solid state as a dimeric species with five-coordinate thorium metal centers, but in ambient-temperature solution in noncoordinating solvents it exists in a monomer–dimer equilibrium as shown in eq 1.[15]

$$Th_2(OCH\text{-}i\text{-}Pr_2)_8 \rightleftharpoons 2Th(OCH\text{-}i\text{-}Pr_2)_4 \qquad (1)$$

We now report a more detailed investigation into the solution properties of $Th_2(OCH$-*i*-$Pr)_8$ together with the isolation and structural characterization of five- and six-coordinate monomeric Lewis base adducts.

Results and Discussion

Synthesis and Reactivity. Reaction of the metallacyclic species $[(Me_3Si)_2N]_2Th[N(SiMe_3)(SiMe_2CH_2)]$ (**1**) with 4 equiv of diisopropylmethanol in toluene, followed by solvent removal and low-temperature crystallization from hexane, leads to the isolation of colorless crystals (**2**) in 67% yield (eq 2). Mi-

$$[(Me_3Si)_2N]_2Th[N(SiMe_3)(SiMe_2CH_2)] + 4HOR \rightarrow \;^1/_2\underset{\mathbf{2}}{Th_2(OR)_8} + 3HN(SiMe_3)_2 \qquad (2)$$

$$R = CH\text{-}i\text{-}Pr_2$$

---

(7) (a) Hitchcock, P. B.; Lappert, M. F.; Singh, A. *J. Chem. Soc., Chem. Commun.* **1983**, 1499. (b) Van der Sluys, W. G.; Burns, C. J.; Huffman, J. C.; Sattelberger, A. P. *J. Am. Chem. Soc.* **1988**, *110*, 5924. (c) Lappert, M. F.; Singh, A.; Smith, R. G. *Inorg. Synth.* **1990**, *27*, 164. (d) Deacon, G. B.; Hitchcock, P. B.; Holmes, S. A.; Lappert, M. F.; MacKinnon, P.; Newnham, R. H. *J. Chem. Soc., Chem. Commun.* **1989**, 935. (e) Stecher, H. A.; Sen, A.; Rheingold, A. L. *Inorg. Chem.* **1988**, *27*, 1130.

(8) Barnhart, D. M.; Clark, D. L.; Gordon, J. C.; Huffman, J. C.; Vincent, R. L.; Watkin, J. G.; Zwick, B. D. *Inorg. Chem.* **1994**, *33*, 3487.

(9) (a) Evans, W. J.; Boyle, T. J.; Ziller, J. W. *Organometallics* **1993**, *12*, 3998. (b) Evans, W. J.; Boyle, T. J.; Ziller, J. W. *J. Am. Chem. Soc.* **1993**, *115*, 5084. (c) Evans, W. J.; Sollberger, M. S.; Ziller, J. W. *J. Am. Chem. Soc.* **1993**, *115*, 4120. (d) Bradley, D. C.; Chudzynska, H.; Hursthouse, M. B.; Motevalli, M. *Polyhedron* **1991**, *10*, 1049. (e) Biagini, P.; Lugli, G.; Abis, L.; Millini, R. *J. Organomet. Chem.* **1994**, *474*, C16. (f) Veith, M.; Hans, J.; Stahl, L.; May, P.; Huch, V.; Sebald, A. *Z. Naturforsch.* **1991**, *46B*, 403. (g) Schumann, H.; Kociok-Kohn, G.; Loebel, J. *Z. Anorg. Allg. Chem.* **1990**, *581*, 69. (h) Clark, D. L.; Watkin, J. G. *Inorg. Chem.* **1993**, *32*, 1766. (i) Heeres, H. J.; Teuben, J. H.; Rogers, R. D. *J. Organomet. Chem.* **1989**, *364*, 87. (j) Evans, W. J.; Deming, T. J.; Olofson, J. M.; Ziller, J. W. *Inorg. Chem.* **1989**, *28*, 4027. (k) Burns, C. J.; Sattelberger, A. P. *Inorg. Chem.* **1988**, *27*, 3692. (l) Cotton, F. A.; Marler, D. O.; Schwotzer, W. *Inorg. Chem.* **1984**, *23*, 4211. (m) Cotton, F. A.; Marler, D. O.; Schwotzer, W. *Inorg. Chim. Acta* **1984**, *85*, L31. (n) Cotton, F. A.; Marler, D. O.; Schwotzer, W. *Inorg. Chim. Acta* **1984**, *95*, 207. (o) Eller, P. G.; Vergamini, P. J. *Inorg. Chem.* **1983**, *22*, 3184. (p) Evans, W. J.; Sollberger, M. S. *Inorg. Chem.* **1988**, *27*, 4417. (q) Evans, W. J.; Sollberger, M. S.; Hanusa, T. P. *J. Am. Chem. Soc.* **1988**, *110*, 1841. (r) Evans, W. J.; Deming, T. J.; Ziller, J. W. *Organometallics* **1989**, *8*, 1581. (s) Evans, W. J.; Olofson, J. M.; Ziller, J. W. *J. Am. Chem. Soc.* **1990**, *112*, 2308.

(10) (a) Evans, W. J.; Golden, R. E.; Ziller, J. W. *Inorg. Chem.* **1991**, *30*, 4963. (b) McGeary, M. J.; Coan, P. S.; Folting, K.; Streib, W. E.; Caulton, K. G. *Inorg. Chem.* **1991**, *30*, 1723. (c) Gradeff, P. S.; Yunlu, K.; Gleizes, A.; Galy, J. *Polyhedron* **1989**, *8*, 1001.

(11) (a) Stecher, H. A.; Sen, A.; Rheingold, A. L. *Inorg. Chem.* **1989**, *28*, 3280. (b) Hitchcock, P. B.; Lappert, M. F.; MacKinnon, I. A. *J. Chem. Soc., Chem. Commun.* **1988**, 1557. (c) Stewart, J. L.; Andersen, R. A. *J. Chem. Soc., Chem. Commun.* **1987**, 1846. (d) Baudin, C.; Ephritikhine, M. *J. Organomet. Chem.* **1989**, *364*, C1.

(12) (a) Herrmann, W. A.; Anwander, R.; Scherer, W. *Chem. Ber.* **1993**, *126*, 1533. (b) Sen, A.; Stecher, H. A.; Rheingold, A. L. *Inorg. Chem.* **1992**, *31*, 473. (c) Baudin, C.; Baudry, D.; Ephritikhine, M.; Lance, M.; Navaza, A.; Nierlich, M.; Vigner, J. *J. Organomet. Chem.* **1991**, *415*, 59. (d) Wedler, M.; Gilje, J. W.; Pieper, U.; Stalke, D.; Noltemeyer, M.; Edelman, F. T. *Chem. Ber.* **1991**, *124*, 1163. (e) Herrmann, W. A.; Anwander, R.; Kleine, M.; Scherer, W. *Chem. Ber.* **1992**, *125*, 1971.

(13) (a) Bradley, D. C.; Chudzynska, H.; Hursthouse, M. B.; Motevalli, M.; Wu, R. *Polyhedron* **1994**, *13*, 1. (b) Bradley, D. C.; Chudzynska, H.; Hursthouse, M. B.; Motevalli, M. *Polyhedron* **1994**, *13*, 7. (c) Bradley, D. C.; Chudzynska, H.; Hursthouse, M. B.; Motevalli, M.; Wu, R. *Polyhedron* **1993**, *12*, 2955. (d) Bradley, D. C.; Chudzynska, H.; Hursthouse, M. B.; Motevalli, M. *Polyhedron* **1993**, *12*, 1907. (e) Bradley, D. C.; Chudzynska, H.; Hammond, M. E.; Hursthouse, M. B.; Motevalli, M.; Wu, R. *Polyhedron* **1992**, *11*, 375. (f) Knosel, F.; Roesky, H. W.; Edelman, F. *Inorg. Chim. Acta* **1987**, *139*, 187. (g) Larson, E. M.; Eller, P. G.; Larson, A. C. *Lanthanide Actinide Res.* **1986**, *1*, 307. (h) Andersen, R. A. *Inorg. Nucl. Chem. Lett.* **1979**, *15*, 57.

(14) $[Nd(OCH$-*i*-$Pr_2)_3(THF)]_2$, $[Nd(OCH$-*i*-$Pr_2)_3(py)]_2$, and $\{[Nd(OCH$-*i*-$Pr_2)_3]_2(\mu$-$DME)\}_n$: Barnhart, D. M.; Clark, D. L.; Huffman, J. C.; Vincent, R. L.; Watkin, J. G. *Inorg. Chem.* **1993**, *32*, 4077.

(15) Clark, D. L.; Huffman, J. C.; Watkin, J. G. *J. Chem. Soc., Chem. Commun.*, **1992**, 266.

croanalytical data were consistent with the formulation of **2** as a homoleptic thorium alkoxide species. An X-ray crystallographic study of **2** (*vide infra*) showed the presence of a dimeric structure in the solid state, and this structural study provides the first example of a crystallographically characterized homoleptic thorium alkoxide complex. However, ^{1}H NMR spectra of **2** in benzene-d_6 or toluene-d_8 solution are consistent with the presence of a monomer–dimer equilibrium between **2** and its monomer $Th(OCH\text{-}i\text{-}Pr_2)_4$ (**3**) as shown in eq 1. A detailed discussion of this equilibrium process is presented in the Spectroscopic Characterization section. **2** is moderately soluble in hexane, benzene, and toluene but reacts with donor solvents to produce monomeric adducts as described below.

Addition of Lewis bases to hydrocarbon solutions of $Th_2(OCH\text{-}i\text{-}Pr_2)_8$ (**2**) leads to cleavage of the dimeric structure and the formation of monomeric Lewis base adducts. Thus the addition of an excess of DME (DME = 1,2-dimethoxyethane) to a toluene solution of **2**, followed by crystallization from hexane, allows the isolation of colorless crystals of the adduct $Th(OCH\text{-}i\text{-}Pr_2)_4(DME)$ (**4**) in 73% yield (eq 3). Microanalytical data support the proposed formulation.

$$Th_2(OR)_8 + 2DME \rightarrow \underset{\mathbf{4}}{2Th(OR)_4(DME)} \tag{3}$$

$$R = CH\text{-}i\text{-}Pr_2$$

In a similar manner, the addition of an excess of pyridine to **2** allows the isolation, following low-temperature crystallization from hexane, of the bis(pyridine) adduct $Th(OCH\text{-}i\text{-}Pr_2)_4(py)_2$ (**5**) in 65% yield (eq 4). ^{1}H NMR integration and microanalytical data are both in agreement with the formulation of **5** with two molecules of coordinated pyridine.

$$Th_2(OR)_8 + 4py \rightarrow \underset{\mathbf{5}}{2Th(OR)_4(py)_2} \tag{4}$$

$$R = CH\text{-}i\text{-}Pr_2$$

In an effort to produce a five-coordinate rather than a six-coordinate monomeric complex, $Th_2(OR)_8$ (**2**) was treated with 1 equiv per thorium atom of the bulky Lewis base quinuclidine (quin). The mono(quinuclidine) adduct $Th(OCH\text{-}i\text{-}Pr_2)_4(quin)$ (**6**) was successfully isolated from the reaction mixture as colorless crystals in 63% yield (eq 5). **6** is found to be soluble in hexane, benzene, and toluene.

$$Th_2(OR)_8 + 2quin \rightarrow \underset{\mathbf{6}}{2Th(OR)_4(quin)} \tag{5}$$

$$R = CH\text{-}i\text{-}Pr_2$$

To provide a site for future alkali-metal salt metathesis reactions, attempts were made to derivatize the tetrakis(alkoxide) framework by replacing one of the alkoxide ligands with a halide moiety. Trimethylsilyl iodide was found to be a suitable reagent for this purpose, and the room-temperature reaction between $Th(OR)_4(py)_2$ (**5**) and 1 equiv of Me_3SiI produced the monoiodide derivative $ThI(OR)_3(py)_2$ (**7**) in excellent yield (eq 6). **7** is soluble in hexane, benzene, and toluene, and may be conveniently recrystallized from hexane at −40 °C.

$$Th(OR)_4(py)_2 + Me_3SiI \rightarrow \underset{\mathbf{7}}{ThI(OR)_3(py)_2} + Me_3SiOR \tag{6}$$

$$R = CH\text{-}i\text{-}Pr_2$$

Table 1. Summary of Crystallographic Data[a]

	2	**6**	**7**
empirical formula	$C_{56}H_{120}O_8Th_2$	$C_{35}H_{73}NO_4Th$	$C_{31}H_{55}IN_2O_3Th$
color, habit	colorless	clear block	clear block
cryst dimens, mm^3	0.12 × 0.32 × 0.32	0.2 × 0.2 × 0.3	0.15 × 0.15 × 0.18
space group	$P2_1/n$	Cc	$P\bar{1}$
cell dimens			
a, Å	12.115(2)	18.778(3)	9.691(2)
b, Å	20.820(3)	11.391(2)	11.739(2)
c, Å	13.002(2)	20.538(3)	17.006(3)
α, deg			77.63(3)
β, deg	100.62(1)	113.51(2)	75.34(3)
γ, deg			72.41(3)
vol, Å^3	3223.4	4028.4	1764.1
Z (molecules/cell)	2	4	2
fw	1385.66	822.4	862.7
d_{calcd}, g cm^{-3}	1.428	1.356	1.624
abs coeff, cm^{-1}	35.638	38.62	52.68
λ(Mo Kα)	0.710 69	0.710 73	0.710 73
temp, °C	−170	−70	−70
2θ range, deg	6.0−45.0	2.0−50.0	2.0−50.0
no. of measd reflns	7246	8201	6609
no. of unique intens	4212	3500	5790
no. of obsd reflns	2640 ($F > 2.33\sigma(F)$)	3247 ($F > 4.00\sigma(F)$)	5348 ($F > 4.00\sigma(F)$)
$R(F)$[b]	0.0503	0.0400	0.0405
$R_w(F)$[c]	0.0484	0.0482	0.0508
goodness-of-fit	1.217	1.51	2.96

[a] **2** = $[Th(OCH\text{-}i\text{-}Pr_2)_4]_2$, **6** = $Th(OCH\text{-}i\text{-}Pr_2)_4(quin)$, and **7** = $ThI(OCH\text{-}i\text{-}Pr_2)_3(py)_2$. [b] $R(F) = \sum||F_o| - |F_c||/\sum|F_o|$. [c] $R_w(F) = [\sum w(|F_o| - |F_c|)^2/\sum w|F_o|^2]^{1/2}$; $w = 1/\sigma^2(|F_o|)$.

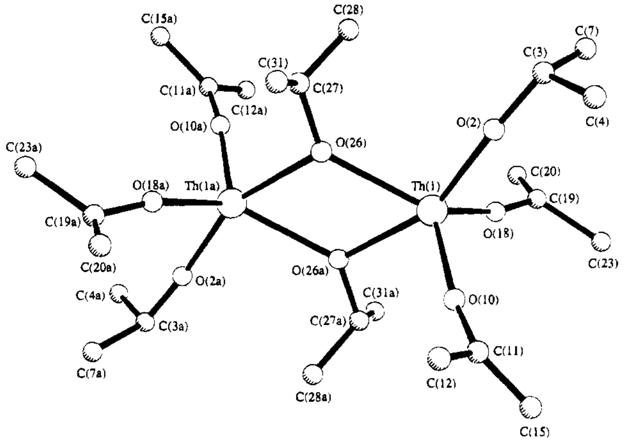

Figure 1. Ball-and-stick view of the molecular structure of $Th_2(OCH\text{-}i\text{-}Pr_2)_8$ (**2**) emphasizing the fused trigonal bipyramidal coordination geometry and showing the atom numbering scheme used in the tables. Methyl carbons of the $OCH\text{-}i\text{-}Pr_2$ ligands are omitted for clarity.

Solid State and Molecular Structures. Three thorium alkoxide complexes have been characterized by X-ray diffraction studies during the course of this work, namely $Th_2(OCH\text{-}i\text{-}Pr_2)_8$ (**2**), $Th(OCH\text{-}i\text{-}Pr_2)_4(quin)$ (**6**) and $ThI(OCH\text{-}i\text{-}Pr_2)_3(py)_2$ (**7**). Data collection and processing parameters for compounds **2**, **6**, and **7** are listed in Table 1.

$Th_2(OCH\text{-}i\text{-}Pr_2)_8$ (2). Crystals of **2** were grown by slow cooling of a concentrated hexane solution to −40 °C. A ball-and-stick view of the molecular structure of **2** showing the numbering scheme used in the tables is presented in Figure 1. Selected fractional atomic coordinates and isotropic thermal parameters are given in Table 2, while selected bond lengths and angles are presented in Table 3. **2** crystallizes in the monoclinic space group $P2_1/n$ with two molecules per unit cell which reside on centers of inversion. Each thorium atom adopts a distorted trigonal bipyramidal geometry, and the Th_2O_8 core can be viewed as two ThO_5 trigonal bipyramids joined along a

Table 2. Selected Fractional Coordinates and Isotropic Thermal Parameters[a] (Å^2) for $Th_2(OCH\text{-}i\text{-}Pr_2)_8$ (**2**)

	10^4x	10^4y	10^4z	10^2B_{iso}
Th(1)	5967(1)	647.5(3)	5942.8(5)	15
O(2)	7158(10)	1314(5)	5493(9)	26
C(3)	8059(16)	1706(8)	5313(15)	31
C(4)	7878(17)	2421(8)	5616(19)	38
C(7)	9157(16)	1421(10)	5847(16)	36
O(10)	4934(10)	1328(5)	6559(9)	24
C(11)	4388(30)	1880(14)	6873(18)	86
C(12)	3680(33)	2198(16)	6179(19)	102
C(15)	4506(17)	1915(9)	8030(16)	36
O(18)	7169(11)	198(6)	7165(9)	33
C(19)	8109(26)	−41(13)	7821(21)	83
C(20)	8505(28)	−600(18)	7719(24)	118
C(23)	8316(21)	343(12)	8898(17)	49
O(26)	5291(9)	290(5)	4178(8)	17
C(27)	5627(19)	390(9)	3203(14)	33
C(28)	6868(15)	336(9)	3329(14)	29
C(31)	5006(15)	968(9)	2648(12)	26

[a] Isotropic values for those atoms refined anisotropically are calculated by using the formula given by: Hamilton, W. C. *Acta Crystallogr.* **1959**, *12*, 609.

Table 3. Selected Bond Distances (Å) and Angles (deg) for $Th_2(OCH\text{-}i\text{-}Pr_2)_8$ (**2**)

Th(1)−Th(1a)	4.081(3)	Th(1)−O(2)	2.160(11)
Th(1)−O(10)	2.141(11)	Th(1)−O(18)	2.161(11)
Th(1)−O(26)	2.408(10)	Th(1)−O(26a)	2.463(11)
O(2)−C(3)	1.416(21)	O(10)−C(11)	1.424(25)
O(18)−C(19)	1.383(26)	O(26)−C(27)	1.417(21)

O(2)−Th(1)−O(10)	98.2(4)	O(2)−Th(1)−O(18)	94.8(5)
O(2)−Th(1)−O(26a)	158.2(4)	O(2)−Th(1)−O(26)	93.9(4)
O(10)−Th(1)−O(18)	111.8(4)	O(10)−Th(1)−O(26a)	98.7(4)
O(10)−Th(1)−O(26)	116.2(4)	O(18)−Th(1)−O(26a)	91.7(4)
O(18)−Th(1)−O(26)	129.2(4)	O(26)−Th(1)−O(26a)	66.2(4)
Th(1)−O(2)−C(3)	171.5(11)	Th(1)−O(10)−C(11)	167.5(17)
Th(1)−O(18)−C(19)	167.4(19)	Th(1)−O(26)−Th(1a)	113.8(4)
Th(1a)−O(26)−C(27)	109.7(10)	Th(1)−O(26)−C(27)	134.7(11)

common axial−equatorial edge. This fused trigonal bipyramidal geometry shows a striking similarity to structures previously observed in some transition metal,[16] lanthanide,[14] and actinide[17] alkoxide and amido complexes. The three equatorial bonds are distorted from the ideal (120°) trigonal angles, the actual values being 129.2(4), 111.8(4) and 116.2(4)°, yet the trigonal ThO_3 unit is nearly planar. The axial O−Th−O unit is distorted (158.2°) from the idealized 180°, and this distortion may be due to steric demands in the bridge. Terminal Th−O distances average 2.154(11) Å, and are comparable to the terminal Th−O distances of 2.154(8), 2.183(8), 2.155(8), 2.172(10), and 2.170(9) Å observed in $[(\eta\text{-}C_5Me_5)_2Th(\mu\text{-}O_2C_2Me_2)]_2$,[18] $Th(O\text{-}t\text{-}Bu)_4(py)_2$,[9h] $Na[Th_2(O\text{-}t\text{-}Bu)_9]$,[9h] $Th_4(O\text{-}i\text{-}Pr)_{16}(py)_2$,[5d] and $Th_2(OCHEt_2)_8(py)_2$,[5d] respectively. The corresponding Th−O−C angles are large, and range from 167.4 to 171.5°. Th−O distances for the bridging ligands (2.436(11) Å average) are, as expected, longer than those for terminal ligands, and are comparable to the distances of 2.464(7), 2.420(10), and 2.427(5) Å found for the bridging alkoxide ligands in $Na[Th_2(O\text{-}t\text{-}Bu)_9]$,[9h] $Th_4(O\text{-}i\text{-}Pr)_{16}(py)_2$,[5d] and $Th_2(OCHEt_2)_8(py)_2$,[5d] respectively. A Th−Th distance of 4.081(3) Å and the lack of valence electrons precludes any metal−metal bonding interaction.

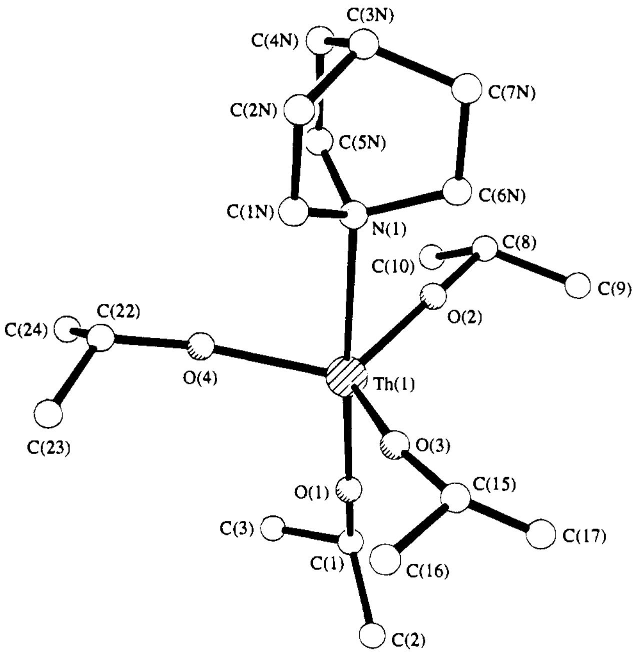

Figure 2. Ball-and-stick view of the molecular structure of $Th(OCH\text{-}i\text{-}Pr_2)_4(quin)$ (**6**), showing the atom numbering scheme used in the tables. Methyl carbons of the $OCH\text{-}i\text{-}Pr_2$ ligands are omitted for clarity.

Table 4. Selected Fractional Coordinates and Equivalent Isotropic Displacement Coefficients (Å^2) for $Th(OCH\text{-}i\text{-}Pr_2)_4(quin)$ (**6**)

	10^4x	10^4y	10^4z	$10^3U(eq)$[a]
Th(1)	−124(4)	8492(1)	−847(4)	28(1)
N(1)	−493(7)	10404(9)	−1705(6)	37(2)
C(1N)	−1041(10)	10160(13)	−2474(9)	63(2)
C(2N)	−1239(11)	11235(13)	−2931(10)	67(2)
C(3N)	−826(8)	12242(11)	−2498(7)	42(2)
C(4N)	37(8)	12017(12)	−2193(8)	45(2)
C(5N)	209(8)	10938(11)	−1718(7)	39(2)
C(6N)	−87710)	11303(11)	−1428(9)	54(2)
C(7N)	−1092(10)	12410(13)	−1911(9)	61(2)
O(1)	221(7)	7068(8)	−97(7)	58(2)
C(1)	627(11)	6289(13)	465(10)	70(2)
C(2)	23(9)	5438(12)	552(9)	54(2)
C(3)	1284(10)	5767(14)	346(10)	73(2)
O(2)	516(6)	9849(8)	−102(6)	39(2)
C(8)	977(9)	10704(11)	413(9)	53(2)
C(9)	686(10)	10901(12)	1015(9)	53(2)
C(10)	1835(9)	10159(13)	724(9)	64(2)
O(3)	−1372(7)	8288(8)	−1223(7)	54(2)
C(15)	−2139(11)	8239(16)	−1255(12)	89(2)
C(16)	−2631(10)	7378(15)	−1857(10)	79(2)
C(17)	−2207(12)	8313(16)	−629(11)	88(2)
O(4)	327(7)	7885(7)	−1609(6)	50(2)
C(22)	490(10)	7370(13)	−2176(9)	66(2)
C(23)	−36(15)	6360(16)	−2563(15)	99(2)
C(24)	1320(10)	7048(13)	−1893(10)	68(2)

[a] Equivalent isotropic *U* defined as one third of the trace of the orthogonalized $\mathbf{U}_{ij}$ tensor.

$Th(OCH\text{-}i\text{-}Pr_2)_4(quin)$ (6). Crystals of $Th(OCH\text{-}i\text{-}Pr_2)_4(quin)$ (**6**) were grown from a concentrated hexane solution at −40 °C. A ball-and-stick representation of the solid state structure of **6** is shown in Figure 2. Selected fractional atomic coordinates and isotropic thermal parameters are listed in Table 4, while selected bond lengths and angles are presented in Table 5. The overall molecular structure of **6** consists of a central thorium atom coordinated in a trigonal bipyramidal fashion by four alkoxide and one quinuclidine ligand, with the nitrogen-containing base occupying an axial site. Th−O bond lengths

---

(16) (a) $[Mo(O\text{-}i\text{-}Pr)_4]_2$: Chisholm, M. H.; Cotton, F. A.; Extine, M. W.; Reichert, W. W. *Inorg. Chem.* **1978**, *17*, 2944. (b) $[Mo(O\text{-}i\text{-}Pr)_3(NO)]_2$: Chisholm, M. H.; Cotton, F. A.; Extine, M. W.; Kelly, R. L. *J. Am. Chem. Soc.* **1978**, *100*, 3354.

(17) (a) $U_2(NEt_2)_8$: Reynolds, J. G.; Zalkin, A.; Templeton, D. H.; Edelstein, N. M.; Templeton, L. K. *Inorg. Chem.* **1976**, *15*, 2498. (b) $U_2(O\text{-}i\text{-}Pr)_6[N(SiMe_3)_2]_2$: Barnhart, D. M.; Sauer, N. N.; Watkin, J. G. Manuscript in preparation.

(18) Manriquez, J. M.; Fagan, P. J.; Marks, T. J.; Day, C. S.; Day, V. W. *J. Am. Chem. Soc.* **1978**, *100*, 7112.

Table 5. Selected Bond Distances (Å) and Angles (deg) for $Th(OCH\text{-}i\text{-}Pr_2)_4(quin)$ (**6**)

Th(1)−N(1)	2.712(11)	Th(1)−O(1)	2.152(12)
Th(1)−O(2)	2.169(10)	Th(1)−O(3)	2.169(14)
Th(1)−O(4)	2.168(17)	N(1)−C(1N)	1.528(19)
N(1)−C(5N)	1.461(21)	N(1)−C(6N)	1.490(22)
N(1)−Th(1)−O(1)	175.4(4)	Th(1)−O(1)−C(1)	165.5(10)
N(1)−Th(1)−O(2)	79.2(3)	Th(1)−O(2)−C(8)	176.6(8)
N(1)−Th(1)−O(3)	84.0(4)	Th(1)−O(3)−C(15)	162.8(13)
O(1)−Th(1)−O(2)	96.2(5)	Th(1)−O(4)−C(22)	169.3(10)
O(1)−Th(1)−O(3)	98.5(5)	O(2)−Th(1)−O(3)	122.9(6)
N(1)−Th(1)−O(4)	81.9(5)	O(1)−Th(1)−O(4)	100.6(5)
O(2)−Th(1)−O(4)	118.1(6)	O(3)−Th(1)−O(4)	112.7(5)

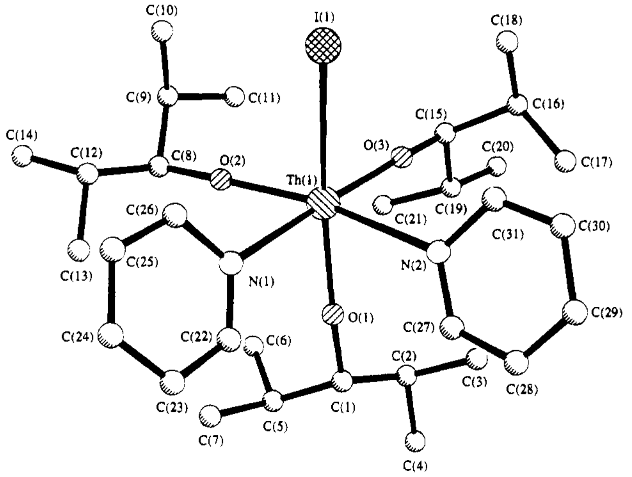

Figure 3. Ball-and-stick view of the molecular structure of $ThI(OCH\text{-}i\text{-}Pr_2)_3(py)_2$ (**7**), showing the atom numbering scheme used in the tables.

average 2.165(17) Å, with no significant differences between $Th{-}O_{axial}$ and $Th{-}O_{equatorial}$ bond lengths. This average Th−O distance is directly comparable to those listed above for **2** and related complexes. The Th−N distance of 2.712(11) Å is similar to the average Th−N distances of 2.679(8), 2.752(7), 2.740(14), and 2.730(6) Å seen in $Th(O\text{-}2,6\text{-}Me_2C_6H_3)_4(py)_2$,[19] $Th(O\text{-}t\text{-}Bu)_4(py)_2$,[9h] $Th_4(O\text{-}i\text{-}Pr)_{16}(py)_2$,[5d] and $Th_2(OCHEt_2)_8(py)_2$,[5d] respectively, while being slightly longer than the 2.61(1) Å observed for the chelating 2-(6-methylpyridyl)methyl ligand in $Th(O\text{-}2,6\text{-}t\text{-}Bu_2C_6H_3)_2(CH_2\text{-}py\text{-}6\text{-}Me)_2$.[20] The axial N(1)−Th(1)−O(1) angle is almost linear (175.4(4)°), while the three O−Th−O angles in the equatorial plane sum to 353.7°, indicating near-planarity of the thorium atom and equatorial oxygen atoms. As is the case with virtually all terminal thorium alkoxide ligands, Th−O−C angles are very obtuse at 168.6° (average). Examples of structurally characterized mononuclear actinide complexes exhibiting a five-coordinate geometry are rare, being limited to the salt complexes $[Li(THF)_4][An(O\text{-}2,6\text{-}i\text{-}Pr_2C_6H_3)_5]$ (An = U, Th),[21] $[K_2(THF)_4][U(NH\text{-}2,6\text{-}i\text{-}Pr_2C_6H_3)_5]$,[22] and $[Li][UMe(OCH\text{-}t\text{-}Bu_2)_4]$.[11c]

Table 6. Selected Fractional Coordinates and Equivalent Isotropic Displacement Coefficients ($Å^2$) for $ThI(OCH\text{-}i\text{-}Pr_2)_3(py)_2$ (**7**)

	10^5x	10^5y	10^5z	$10^4U(eq)^a$
Th(1)	22792(3)	−23267(3)	−26155(2)	179(1)
I(1)	1282(7)	3231(5)	−30326(4)	349(2)
O(1)	42466(64)	−37756(52)	−26136(35)	249(21)
O(3)	9804(63)	−31521(52)	−30477(34)	269(21)
O(2)	14370(67)	−24550(55)	−13227(37)	240(24)
N(1)	39805(72)	−10197(63)	−23438(44)	228(25)
N(2)	38232(91)	−17575(69)	−41773(45)	312(31)
C(1)	53972(90)	−48843(77)	−25810(53)	234(31)
C(2)	51324(96)	−57669(83)	−30258(58)	291(33)
C(5)	55991(94)	−53658(85)	−16935(58)	293(34)
C(8)	8762(97)	−26445(78)	−4580(53)	263(32)
C(9)	−8023(103)	−25360(91)	−2865(53)	329(36)
C(12)	13142(97)	−18185(81)	−358(52)	272(32)
C(15)	1597(103)	−38224(87)	−32486(59)	331(35)
C(16)	−1028(101)	−33257(84)	−41321(58)	319(35)
C(19)	8847(108)	−51644(87)	−30945(65)	375(37)
C(22)	54035(110)	−14296(95)	−24388(63)	356(39)
C(23)	63249(128)	−9167(106)	−22182(64)	448(46)
C(24)	56732(146)	1569(109)	−18880(70)	499(53)
C(25)	41685(148)	6015(105)	−17778(69)	506(50)
C(26)	33284(130)	317(89)	−20215(59)	370(41)
C(27)	52432(107)	−22304(96)	−43893(61)	359(39)
C(28)	60923(133)	−20507(116)	−51579(64)	493(48)
C(29)	54242(153)	−13505(111)	−57643(67)	536(55)
C(30)	38968(159)	−8152(105	−55788(69)	578(54)
C(31)	31214(132)	−10328(90)	−47945(62)	405(42)

[a] Equivalent isotropic U defined as one third of the trace of the orthogonalized $\mathbf{U}_{ij}$ tensor.

Table 7. Selected Bond lengths (Å) and Angles (deg) for $ThI(OCH\text{-}i\text{-}Pr_2)_3(py)_2$ (**7**)

Th(1)−I(1)	3.226(1)	Th(1)−O(1)	2.137(5)
Th(1)−O(3)	2.139(8)	Th(1)−O(2)	2.132(5)
Th(1)−N(1)	2.739(9)	Th(1)−N(2)	2.752(7)
O(1)−C(1)	1.437(9)	O(3)−C(15)	1.414(14)
O(2)−C(8)	1.427(10)		
I(1)−Th(1)−O(1)	160.2(2)	I(1)−Th(1)−O(3)	91.4(1)
O(1)−Th(1)−O(3)	99.5(2)	I(1)−Th(1)−O(2)	94.4(1)
O(1)−Th(1)−O(2)	98.8(2)	O(3)−Th(1)−O(2)	104.3(2)
I(1)−Th(1)−N(1)	82.7(1)	O(1)−Th(1)−N(1)	83.8(2)
O(3)−Th(1)−N(1)	169.4(2)	O(2)−Th(1) −N(1)	84.9(2)
I(1)−Th(1)−N(2)	82.9(1)	O(1)−Th(1)−N(2)	80.1(2)
O(3)−Th(1)−N(2)	92.5(3)	O(2)−Th(1)−N(2)	163.0(3)
N(1)−Th(1)−N(2)	78.1(3)	Th(1)−O(1)−C(1)	169.9(6)
Th(1)−O(3)−C(15)	172.5(5)	Th(1)−O(2)−C(8)	175.1(6)

$ThI(OCH\text{-}i\text{-}Pr_2)_3(py)_2$ (7). Crystals of $ThI(OCH\text{-}i\text{-}Pr_2)_3(py)_2$ (**7**) were grown from hexane solution at −40 °C. A ball-and-stick view of the solid state structure of **7** is shown in Figure 3. Selected fractional atomic coordinates are given in Table 6, while selected bond lengths and angles are presented in Table 7. **7** exhibits a facial pseudooctahedral geometry in the solid state. The three Th−O bond lengths are virtually identical (2.136(8) Å (average)), with no significant differences being seen for the alkoxide ligands *trans* to pyridine compared with the alkoxide *trans* to iodine. These Th−O distances are again very similar to those observed for **2** and **6** and the related thorium alkoxide complexes referenced above. Th−N bond distances of 2.746(9) Å (average) are directly comparable to the Th−N distance found in $Th(OR)_4(quin)$ (**6**) (*vide supra*). The Th−I distance of 3.226(1) Å is, as expected, somewhat longer than typical U(IV)−I distances (*e.g.* 3.041(1) Å in $(\eta^3\text{-}C_9H_7)_3UI$[23] and 2.996(3) and 3.027(3) Å in $UI_4(tmu)_2$, tmu = tetramethylurea[24]), but is also significantly longer than the Th−I distances of 3.045 and 3.099(2) Å observed in $(\eta\text{-}C_5Me_5)_2ThI\text{-}Ru(CO)_2Cp$[25] and $Th_2I_4(O\text{-}i\text{-}Pr)_4(HO\text{-}i\text{-}Pr)_2$,[26] which would

---

(19) Berg, J. M.; Clark, D. L.; Huffman, J. C.; Morris, D. E.; Sattelberger, A. P.; Streib, W. E.; Van der Sluys, W. G.; Watkin, J. G. *J. Am Chem. Soc.* **1992**, *114*, 10811.

(20) Beshouri, S. M.; Fanwick, P. E.; Rothwell, I. P.; Huffman, J. C., *Organometallics* **1987**, *6*, 2498.

(21) Blake, P. C.; Lappert, M. F.; Taylor, R. G.; Atwood, J. L.; Zhang, H. *Inorg. Chim. Acta* **1987**, *139*, 13.

(22) Nelson, J. E.; Clark, D. L.; Burns, C. J.; Sattelberger, A. P. *Inorg. Chem.* **1992**, *31*, 1973.

(23) Rebizant, J.; Spirlet, M. R.; Van den Bossche, G.; Goffart, J. *Acta Crystallogr.* **1988**, *44C*, 1710.

(24) DuPreez, J. G. H.; Zeelie, B.; Casellato, U.; Graziani, R. *Inorg. Chim. Acta* **1987**, *129*, 289.

(25) Sternal, R. S.; Brock, C. P.; Marks, T. J. *J. Am. Chem. Soc.* **1985**, *107*, 8270.

(26) Barnhart, D. M.; Burns, C. J.; Frankcom, T. M.; Gordon, P. L.; Sauer, N. N.; Thompson, J. A.; Watkin, J. G. *Inorg. Chem.* **1995**, *34*, 4862.

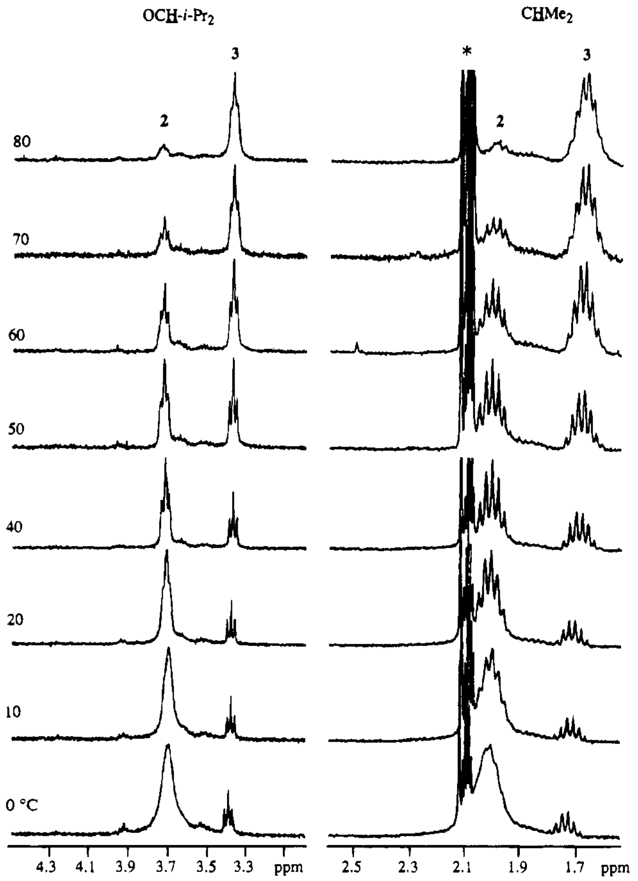

Figure 4. ^{1}H NMR spectrum of the methine region of an equilibrium mixture of $Th_2(OCH\text{-}i\text{-}Pr_2)_8$ (**2**) and monomeric $Th(OCH\text{-}i\text{-}Pr_2)_4$ (**3**) at temperatures from 0 to 80 °C. The resonance marked with an asterisk denotes the ^{1}H impurity in toluene-d_8.

appear to be the only other examples of structurally characterized molecular complexes containing thorium–iodide bonds. Th–O–C angles are almost linear, averaging 172.5°. Angles about the thorium atom are somewhat distorted from ideal octahedral values, the I(1)–Th(1)–O(1) angle having a value of 160.2(2)° and the N(1)–Th(1)–N(2) angle between the two pyridine ligands being reduced from 90° down to 78.1(3)°.

Spectroscopic Characterization. (a) Monomer–Dimer Equilibrium. Ambient temperature (293K) ^{1}H NMR spectra of $Th_2(OCH\text{-}i\text{-}Pr_2)_8$ (**2**) in benzene-d_6 or toluene-d_8 solution reveal the presence of two different alkoxide environments. Figure 4 shows a stack plot of the ^{1}H NMR spectrum of **2** in toluene-d_8 solution at temperatures from 0 to 80 °C, in which the methine regions of the spectrum are expanded. At room temperature (20 °C spectrum) one set of broadened methine resonances is seen at 2.0 and 3.72 ppm and a smaller, sharp set of resonances at 1.75 and 3.38 ppm. Similarly, two overlapping sets of diastereotopic methyl group resonances are seen in the region 1.0–1.2 ppm. Integrated intensities of *ca.* 9:1 for the ratio of these two alkoxide environments precludes any assignment of these resonances to terminal and bridging groups within the dimeric species $Th_2(OCH\text{-}i\text{-}Pr_2)_8$. The relative intensities of the resonances, together with the observation that one set of resonances is broad (presumably due to bridge–terminal exchange) and the other is sharp, is indicative of two separate species in solution at room temperature. The data are consistent with an equilibrium between dimeric $Th_2(OR)_8$ (**2**) and its monomer $Th(OR)_4$ (**3**) taking place in solution at ambient temperatures (eq 1). The broadened set of methine resonances is assigned to the dimeric species **2** and is due to the rapid exchange between bridging and terminal alkoxide ligands. The set of sharp resonances is assigned to monomeric $Th(OR)_4$ (**3**), in which all alkoxide ligands are equivalent at all temperatures.

Further evidence in support of this assignment is obtained from variable temperature NMR experiments. When the sample is heated, the resonances assigned to the dimer (**2**) are seen to decrease, while those assigned to monomeric **3** increase in intensity, consistent with an equilibrium between **2** and **3** in solution (Figure 4). At 80 °C the monomeric complex **3** is the predominant species in solution. When cooled to room temperature, the resonances of the dimer **2** grow back in rapidly, implying a low barrier to dimerization.

When the temperature is lowered, the opposite effect is observed. Resonances due to the monomer **3** decrease in intensity, and at temperatures below 0 °C the dimer is by far the major species present in solution. As the temperature is lowered further, the resonances assigned to the dimer $Th_2(OCH\text{-}i\text{-}Pr_2)_8$ (**2**) are seen to broaden significantly, and eventually each methine resonance can be seen to decoalesce into two separate peaks which integrate in the approximate ratio of 3:1. This observation is explained by the exchange process between terminal and bridging alkoxide ligands being effectively frozen out, resulting in a structure approximating that seen in the solid state (in which terminal and bridging alkoxide ligands are in a 3:1 ratio).

Since the equilibrium process (eq 1) occurs at temperatures close to ambient, this system seemed ideally suited to the application of detailed ^{1}H NMR investigations to determine both the kinetic and thermodynamic parameters for the equilibrium. Initial investigations aimed to determine thermodynamic parameters by measuring relative concentrations of monomer and dimer at a range of temperatures. Since equilibrium is rapidly established even at ambient temperatures and since **2** does not exhibit visible decomposition when heated to 80 °C, we were able to measure the relative concentrations of **2** and **3** at 13 temperatures between 20 and 80 °C. The $OCH\text{-}i\text{-}Pr_2$ methine protons provided a convenient resonance for integration purposes, since this resonance was well-resolved in both monomer and dimer, and existed in a region of the spectrum well away from residual solvent resonances. A plot of $\ln(K_{eq})$ *vs* $1/T$ produced the following parameters: $\Delta H° = 17$ kcal mol^{-1}, $\Delta G°_{298} = 5$ kcal mol^{-1}, and $\Delta S° = 40$ cal mol^{-1} K^{-1}. These values may be compared with those found by Chisholm *et al.* for the dimer–tetramer equilibrium process shown in eq 7,[27] in which $\Delta H° = 21$ kcal mol^{-1}, $\Delta G°_{298} = 4$ kcal mol^{-1}, and $\Delta S° = 56$ cal mol^{-1} K^{-1}.

$$W_4(O\text{-}i\text{-}Pr)_{12} \rightleftharpoons 2W_2(O\text{-}i\text{-}Pr)_6 \qquad (7)$$

A subsequent attempt was made to obtain activation parameters for the equilibrium process by studying the approach to equilibrium at a range of temperatures. Unfortunately, it was found that equilibrium is established too rapidly in this system for any meaningful solution ^{1}H NMR data to be collected. In a typical experiment, an NMR sample was allowed to equilibrate for a prolonged period in a −78 °C bath and was then introduced as rapidly as possible into the NMR instrument. All of the spectra collected subsequently, however, showed a constant ratio of **2**:**3**, indicating that equilibrium had been reached even before the first spectrum had been acquired.

(b) Mononuclear Adducts. Ambient temperature ^{1}H NMR spectra of the DME adduct $Th(OR)_4(DME)$ (**4**) and of the bis(pyridine) adduct $Th(OR)_4(py)_2$ (**5**) reveal only one type of alkoxide ligand environment, suggesting the presence of a rapid

---

(27) Chisholm, M. H.; Clark, D. L.; Hampden-Smith, M. J. *J. Am. Chem. Soc.* **1989**, *111*, 574.

fluxional process which equivalences all alkoxide ligands on the NMR time scale. This is entirely consistent with the behavior we have previously observed in related $Th(OR)_4L_2$ systems, in which we have been unable to freeze out a limiting structure even at −80 °C. Although solid-state structural data for $Th(OR)_4(DME)$ (**4**) could not be obtained, we propose an octahedral solid state geometry by analogy with several structurally characterized six-coordinate thorium alkoxide and aryloxide complexes of the type $Th(OR)_4L_2$.[9h,19] Taking into account the inability of a DME ligand to span *trans* sites in an octahedral complex, we propose the geometry shown schematically in **V** in which the DME ligand occupies two adjacent sites in a *cis* configuration.

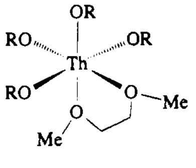

V

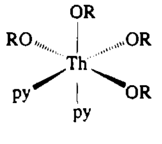

VI

R = CH-*i*-Pr_2

Similarly, consideration of the structures of the crystallographically characterized complexes $Th(O\text{-}2,6\text{-}Me_2C_6H_3)_4(py)_2$,[19] $Th(O\text{-}t\text{-}Bu)_4(py)_2$,[9h] and $ThI(OCH\text{-}i\text{-}Pr_2)_3(py)_2$ (**7**) (*vide supra*) allows us to propose an analogous structure for $Th(OR)_4(py)_2$ (**5**) in which two pyridine ligands occupy *cis* coordination sites within a pseudooctahedral geometry (as shown schematically in **VI**).

Similar fluxional processes are also present in the room-temperature ^1H NMR spectra of the five-coordinate quinuclidine adduct $Th(OR)_4(quin)$ (**6**) and the monoiodide derivative $ThI(OR)_3(py)_2$ (**7**), which each show a single type of alkoxide ligand environment. Static structures, similar to that observed in the solid state, would result in the observation of two alkoxide environments in a 3:1 ratio for **6** and two alkoxide environments in a 2:1 ratio for **7**. Thus we once again propose that rapid fluxional processes are operating in solution at ambient temperature, resulting in equivalence of all alkoxide ligands on the NMR time scale.

Concluding Remarks

We have shown, both in this work and in previous publications,[14,15] that the sterically demanding diisopropylmethoxide ligand can be used successfully in f-element alkoxide chemistry to prepare discrete low-nuclearity complexes which are not susceptible to the progressive oligomerization which has been observed previously in f-element alkoxide complexes containing smaller alkoxide ligands such as methoxide and isopropoxide.[5d] We have prepared and structurally characterized a number of new thorium alkoxide complexes containing diisopropylmethoxide ligation, including $Th_2(OCH\text{-}i\text{-}Pr_2)_8$ (**2**) which provides the first example of a crystallographically characterized homoleptic thorium alkoxide species. We have shown that the dimeric species $Th_2(OCH\text{-}i\text{-}Pr_2)_8$ exists in solution at ambient temperatures in an equilibrium with the monomer $Th(OCH\text{-}i\text{-}Pr_2)_4$ (**3**), and that the relative concentrations of **2** and **3** in solution are highly temperature dependent. We have used this temperature dependence to obtain thermodynamic parameters for the equilibrium process, but unfortunately the very rapid approach to equilibrium, even at low temperatures, has prevented activation parameters from being obtained. Reaction of **2** with a variety of Lewis bases has been shown to produce either trigonal bipyramidal five-coordinate or pseudooctahedral six-coordinate environments around the thorium metal center in the solid state, depending upon the steric requirement of the Lewis base present in the complex.

Experimental Section

General Procedures and Techniques. All manipulations were carried out under an inert atmosphere of oxygen-free UHP grade argon using standard Schlenk techniques, or under oxygen-free helium in a Vacuum Atmospheres glovebox. $[(Me_3Si)_2N]_2Th[N(SiMe_3)(SiMe_2CH_2)]$ was prepared following literature procedures.[28] Diisopropylmethanol and quinuclidine were purchased from Aldrich and used without further purification. Trimethylsilyl iodide (Aldrich) was trap-to-trap distilled and stored in the freezer. Solvents, except for pyridine, were degassed and distilled from Na/K alloy under nitrogen. Pyridine was distilled from CaH_2 under argon. Benzene-d_6 and toluene-d_8 were degassed, dried over Na/K alloy and then trap-to-trap distilled before use. Solvents were taken into the glovebox and a small amount tested with a solution of sodium benzophenone in THF. Solvents that failed to maintain a purple coloration from this test were not used.

NMR spectra were recorded at 22 °C on Brüker AF 250 or WM 300 spectrometers in benzene-d_6 or toluene-d_8. All ^1H NMR chemical shifts are reported in ppm relative to the ^1H impurity in benzene-d_6 or toluene-d_8 set at δ 7.15 or 2.09, respectively. Infrared spectra were recorded on a Perkin-Elmer 1500 spectrophotometer interfaced with a Model 1502 central processor. Elemental analyses were performed on a Perkin-Elmer 2400 CHN analyzer. Elemental analysis samples were prepared and sealed in tin capsules in the glovebox prior to combustion.

$Th_2(OCH\text{-}i\text{-}Pr_2)_8$ (2). To a solution of $[(Me_3Si)_2N]_2Th[N(SiMe_3)(SiMe_2CH_2)]$ (1.00 g, 1.40 mmol) in toluene (100 mL) was added dropwise a solution of diisopropylmethanol (0.66 g, 5.7 mmol) in toluene (10 mL), and the resulting solution stirred at room temperature for 24 h before being stripped to dryness. The off-white solid residue was taken up in 100 mL of hexane and filtered through a Celite pad. The volume of the filtrate was reduced to 25 mL and the solution placed at -40 °C. Colorless crystals were deposited overnight, decanted free from solvent, and allowed to dry. Yield: 0.66 g (67%). ^1H NMR (250 MHz, toluene-d_8): for **2**, δ 3.72 (t, $^3J_{HH}$ = 6 Hz, 1 H, C*H*-*i*-Pr_2), 2.02 (octet, $^3J_{HH}$ = 6 Hz, 2 H, C*H*Me_2), 1.20 (d, $^3J_{HH}$ = 7 Hz, 6 H, CH*Me_2*), 1.07 (d, $^3J_{HH}$ = 7 Hz, 6 H, CH*Me_2*); for **3** δ 3.39 (t, $^3J_{HH}$ = 6 Hz, 1 H, C*H*-*i*-Pr_2), 1.72 (octet, $^3J_{HH}$ = 7 Hz, 2 H, C*H*Me_2), 1.10 (d, $^3J_{HH}$ = 7 Hz, 6 H, CH*Me_2*), 0.99 (d, $^3J_{HH}$ = 7 Hz, 6 H, CH*Me_2*). Anal. Calcd for $C_{28}H_{60}O_4Th$: C, 48.54; H, 8.73. Found: C, 47.76; H, 8.75.

$Th(OCH\text{-}i\text{-}Pr_2)_4(DME)$ (4). In the drybox, 1.00 g (0.72 mmol) of $Th_2(OCH\text{-}i\text{-}Pr_2)_8$ (**2**) was dissolved in 50 mL of toluene and 10 mL of DME added. After the mixture was stirred at room temperature for 6 h, all solvent was removed *in vacuo* to leave a colorless oil. The oil was dissolved in 50 mL of hexane and the volume of the solution reduced to 5 mL. The solution was cooled to -40 °C, producing colorless crystals overnight. These were collected by decantation and pumped dry. Yield: 0.82 g (73%). ^1H NMR (300 MHz, benzene-d_6): δ 3.44 (t, $^3J_{HH}$ = 5 Hz, 2 H, C*H*-*i*-Pr_2), 3.25 (s, 3 H, O*Me*), 3.06 (s, 2 H, OC*H_2*C*H_2*O), 1.84 (octet, $^3J_{HH}$ = 6 Hz, 4 H, C*H*Me_2), 1.20 (d, $^3J_{HH}$ = 6 Hz, 12 H, CH*Me_2*), 1.10 (d, $^3J_{HH}$ = 6 Hz, 12 H, CH*Me_2*). Anal. Calcd for $C_{32}H_{70}O_6Th$: C, 49.09; H, 9.01. Found: C, 49.63, 49.51; H, 8.89, 9.29.

$Th(OCH\text{-}i\text{-}Pr_2)_4(py)_2$ (5). To a solution of 0.41g (0.30 mmol) of $Th_2(OCH\text{-}i\text{-}Pr_2)_8$ (**2**) in 30 mL of hexane was added 95 μL (1.17 mmol) of pyridine. The solution was stirred for 1 h at room temperature and then concentrated to *ca.* 5 mL and placed at −40 °C overnight, after which time a waxy white solid was collected by removal of the mother liquor and pumping to dryness. A second crop was obtained by concentration of the mother liquor, placing it at −40 °C, and repeating the above procedure. Total yield: 0.32 g (65%). ^1H NMR (250 MHz, benzene-d_6): δ 8.71 (m, 2 H, *ortho* py), 6.93 (m, 1 H, *para* py), 6.68 (m, 2 H, *meta* py), 3.48 (t, $^3J_{HH}$ = 5 Hz, 2 H, C*H*-*i*-Pr_2), 1.78 (octet, $^3J_{HH}$ = 4 Hz, 4 H, C*H*Me_2), 1.20 (d, $^3J_{HH}$ = 6 Hz, 12 H, CH*Me_2*), 1.02 (d, $^3J_{HH}$ = 6 Hz, 12 H, CH*Me_2*). IR (cm^{-1}): 1630 (w), 1598 (m),

---

(28) Dormond, A., El Bouadili, A., Aaliti, A., Moise, C. *J. Organomet. Chem.* **1985**, *288*, C1.

1575 (w), 1446 (s), 1366 (s), 1353 (m), 1343 (m), 1312 (w), 1300 (w), 1271 (w), 1216 (w), 1180 (m), 1154 (m), 1139 (s), 1107 (s), 1069 (w), 1047 (w), 1035 (m), 984 (m), 954 (w), 919 (w), 909 (w), 851 (w), 798 (w), 750 (m), 723 (w), 702 (s), 672 (s), 621 (m), 516 (m), 475 (m). Anal. Calcd for $C_{38}H_{70}N_2O_4Th$: C, 53.63; H, 8.29; N, 3.29. Found: C, 51.79; H, 7.20; N, 2.57.

Th(OCH-*i*-Pr$_2$)$_4$(quin) (6). To a solution of 0.70 g (0.51 mmol) of $Th_2(OCH\text{-}i\text{-}Pr_2)_8$ (**2**) in 50 mL of toluene was added dropwise a solution of 0.118 g (1.06 mmol) of quinuclidine in 10 mL of toluene. The mixture was stirred at room temperature for 6 h before being stripped to dryness. The solid was dissolved in 50 mL of hexane and filtered through a Celite pad. The volume of the filtrate was reduced to 10 mL and placed at −40 °C. Colorless crystals were deposited overnight, collected on a frit, and pumped dry. Yield: 0.51 g (63%). ^{1}H NMR (300 MHz, benzene-d_6): δ 3.47 (t, $^3J_{HH}$ = 4 Hz, 4 H, C*H*-*i*-Pr$_2$), 3.14 (m, 6 H, NC*H*$_2$), 1.80 (octet, $^3J_{HH}$ = 6 Hz, 8 H, C*H*Me$_2$), 1.35 (m, 7 H, C*H*$_2$CH and CH$_2$C*H*), 1.18 (d, $^3J_{HH}$ = 6 Hz, 24 H, CH*Me*$_2$), 1.04 (d, $^3J_{HH}$ = 6 Hz, 24 H, CH*Me*$_2$). IR (cm^{-1}): 1401 (w), 1362 (m), 1343 (w), 1317 (w), 1267 (w), 1200 (w), 1178 (m), 1156 (m), 1138 (s), 1103 (s), 1069 (m), 1050 (sh, m), 1016 (s), 987 (s), 952 (m), 918 (w), 908 (w), 853 (w), 799 (m), 782 (m), 721 (w), 670 (s), 638 (m), 624 (m), 510 (m), 475 (m). Anal. Calcd for $C_{35}H_{73}NO_4Th$: C, 52.29; H, 9.15; N, 1.74. Found: C, 53.28; H, 9.02; N, 1.63.

ThI(OCH-*i*-Pr$_2$)$_3$(py)$_2$ (7). A 0.11 g (0.13 mmol) sample of Th(OCH-*i*-Pr$_2$)$_4$(py)$_2$ (**5**) was dissolved in 20 mL of hexanes, and 0.027 g (0.14 mmol) of Me$_3$SiI in 5 mL hexanes was added. The mixture was allowed to stir for 2 h at room temperature, and then all of the solvent was removed *in vacuo*, leaving a white solid. Yield: 0.10 g (92%). Crystalline material was obtained by recrystallization of this solid from hexane at −40 °C. ^{1}H NMR (250 MHz, benzene-d_6): δ 9.09 (m, 4 H, *ortho* py), 6.89 (m, 2 H, *para* py), 6.63 (m, 4 H, *meta* py), 3.63 (t, $^3J_{HH}$ = 6 Hz, 3 H, C*H*-*i*-Pr$_2$), 1.87 (octet, $^3J_{HH}$ = 6 Hz, 6 H, C*H*Me$_2$), 1.17 (d, $^3J_{HH}$ = 8 Hz, 18 H, CH*Me*$_2$), 1.03 (d, $^3J_{HH}$ = 8 Hz, 18 H, CH*Me*$_2$). IR (cm^{-1}): 1628 (m), 1598 (s), 1569 (m), 1486 (sh, s), 1444 (s), 1367 (s), 1342 (m), 1313 (w), 1268 (w), 1221 (sh, m), 1213 (s), 1180 (s), 1159 (sh, m), 1138 (s), 1107 (s), 1069 (m), 1037 (s), 1011 (s), 983 (s), 951 (m), 922 (m), 853 (w), 800 (m), 753 (s), 697 (s), 677 (s), 670 (sh, s), 622 (s), 515 (s), 476 (m). Anal. Calcd for $C_{31}H_{55}IN_2O_3Th$: C, 43.16; H, 6.43; N, 3.25. Found: C, 42.25; H, 5.96; N, 3.27.

Crystallographic Studies. A summary of crystallographic data can be found in Table 1.

Th$_2$(OCH-*i*-Pr$_2$)$_8$ (2). General operating procedures have been described elsewhere.[29] The diffractometer was designed and constructed locally. A Picker four-circle goniostat equipped with a Furnas monochromator (HOG crystal) and Picker X-ray generator is interfaced to a Z80 microprocessor which is controlled by an RS232 serial port on an IBM PC microcomputer. Motors are Slo-Syn stepping motors, and a special top/bottom−left right slit assembly is used to align the crystal. All computations were performed on IBM compatible microcomputer systems. The transparent, air sensitive crystals were manipulated using standard inert atmosphere handling techniques. A suitable crystal was affixed to a goniometer using silicone grease and transferred to the goniostat where it was cooled to −170 °C for characterization and data collection.

A systematic search of a limited hemisphere of reciprocal space located a set of diffraction maxima with symmetry and systematic absences corresponding to the unique monoclinic space group $P2_1/n$ (alternate setting of $P2_1/c$). Subsequent solution and refinement confirmed this choice. Data were collected using standard moving crystal/moving detector techniques with stationary backgrounds at each extreme of the scan. After correction for Lorentz, polarization, and absorption effects, redundant data were averaged to yield a set of unique intensities. The structure was solved by Patterson and Fourier techniques, and refined by full-matrix least-squares methods. All hydrogen atoms were placed in fixed, idealized positions in the final cycle of refinement. A final difference Fourier was featureless, with one large peak (1.54 e/Å^3) at the metal site.

Th(OCH-*i*-Pr$_2$)$_4$(quin) (6). The clear, well-formed crystals were examined in mineral oil under an argon stream. The chosen crystal was affixed to the goniometer head of a CAD4 diffractometer using Apiezon grease and cooled to −70 °C in a nitrogen coldstream. Unit cell parameters were determined from the least-squares refinement of $((\sin\theta)/\lambda)^2$ values for 24 accurately centered reflections with a 2θ range between 27 and 32°. Three reflections were chosen as intensity standards and were measured every 3600 s of X-ray exposure time, and three orientation controls were measured every 250 reflections.

The data were reduced using the Structure Determination Package provided by Enraf-Nonius, and corrected for absorption empirically using high-χ ψ-scans. The solution was from a Patterson map, and refinement was on structure factors. Disorder in the molecule was treated by locating disorder peaks for the terminal isopropyl carbons and refining on the pair of peaks for occupancy. All carbon atoms were treated anisotropically with generated hydrogen atoms used in a riding model. The refinement was limited in that the isotropic temperature factors were fixed before conversion to anisotropic form. An attempt to fix the second set of carbon atoms isotropically and without hydrogens provided a much worse (>6%) refinement. All data refinement calculations were performed using the SHELXTL PLUS suite of computer programs (Siemens Analytical X-ray Instruments, Inc., 1990).

ThI(OCH-*i*-Pr$_2$)$_3$(py)$_2$ (7). A small, colorless crystal measuring 0.15 × 0.15 × 0.18 mm was selected under the microscope, with the crystals immersed in mineral oil under an argon purge. The chosen crystal was affixed to the end of a glass fiber using Apiezon grease and transferred to the goniometer head of an Enraf-Nonius CAD-4 diffractometer with graphite monochromated Mo Kα radiation, where it was cooled in a nitrogen stream to −70 °C. Unit cell parameters were determined from the least-squares refinement of $((\sin\theta)/\lambda)^2$ values for 25 accurately centered reflections having a 2θ range of 28−32°. Three reflections were chosen as intensity standards and were measured every 3600 s of X-ray exposure time, and three orientation controls were measured every 250 reflections.

The data were reduced using the Structure Determination Package provided by Enraf-Nonius and corrected for Lorentz and polarization effects, and an empirical absorption correction based on azimuthal scans was applied. The structure was readily solved by direct methods and subsequent difference Fourier maps and refined using full-matrix least-squares methods. After inclusion of anisotropic thermal parameters for all non-hydrogen atoms and geometrical generation of hydrogen atoms which were constrained to "ride" upon the appropriate carbon atoms, final refinement using 5348 unique observed $[F > 4\sigma(F)]$ reflections converged at $R = 0.0405$, $R_w = 0.0508$. A final difference Fourier contained some residual electron density around the thorium and iodine atoms, the largest peak being 1.47 e/Å^3. All data refinement calculations were performed using the SHELXTL PLUS suite of computer programs (Siemens Analytical X-ray Instruments, Inc., 1990).

Acknowledgment. We acknowledge the Laboratory Directed Research and Development program, the Office of Basic Energy Sciences, Division of Chemical Sciences, U.S. Department of Energy, and the Office of Nuclear Material Production, U.S. Department of Energy, for financial support. Los Alamos National Laboratory is operated by the University of California for the U.S. Department of Energy under Contract No. W-7405-ENG-36.

Supporting Information Available: Tables of fractional atomic coordinates, bond lengths and angles, anisotropic thermal parameters and hydrogen atom coordinates for Th$_2$(OCH-*i*-Pr$_2$)$_8$ (**2**), Th(OCH-*i*-Pr$_2$)$_4$(quin) (**6**) and ThI(OCH-*i*-Pr$_2$)$_3$(py)$_2$ (**7**) (15 pages). Ordering information is given on any current masthead page. Structure factor tables are available from the authors upon request.

IC9505458

---

(29) Chisholm, M. H.; Folting, K. Huffman, J. C.; Kirkpatrick, C. C. *Inorg. Chem.* **1984**, *23*, 1021.